Journal of Molecular Liquids 407 (2024) 125157

Contents lists available at ScienceDirect

Journal of Molecular Liquids

journal homepage: www.elsevier.com/locate/molliq

Hydrogel immobilized microalgae-alginate beads to model the fermentation of phenol-containing wastewater into biohydrogen molecules

Jia Min Woon [a,1], Kuan Shiong Khoo [b,c,1], Mohsin Kazi [d], Mohammad Nur-e-Alam [e], Nurul Tasnim Sahrin [a], Jun Wei Lim [a,f,*], Worapon Kiatkittipong [g,*], Sameh S. Ali [h], Chii-Dong Ho [i], Anwar Usman [j], Boredi Silas Chidi [k], Woei-Yenn Tong [l,*]

[a] HICoE-Centre for Biofuel and Biochemical Research, Institute of Sustainable Energy, Department of Fundamental and Applied Sciences, Universiti Teknologi PETRONAS, 32610 Seri Iskandar, Perak Darul Ridzuan, Malaysia
[b] Department of Chemical Engineering and Materials Science, Yuan Ze University, Taoyuan, Taiwan
[c] Centre for Herbal Pharmacology and Environmental Sustainability, Chettinad Hospital and Research Institute, Chettinad Academy of Research and Education, Kelambakkam 603103, Tamil Nadu, India
[d] Department of Pharmaceutics, College of Pharmacy, POBOX 2457, King Saud University, Riyadh 11451, Kingdom of Saudi Arabia
[e] Department of Pharmacognosy, College of Pharmacy, POBOX 2457, King Saud University, Riyadh 11451, Kingdom of Saudi Arabia
[f] Department of Biotechnology, Saveetha School of Engineering, Saveetha Institute of Medical and Technical Sciences, Saveetha University, Chennai, India
[g] Department of Chemical Engineering, Faculty of Engineering and Industrial Technology, Silpakorn University, Nakhon Pathom 73000, Thailand
[h] Botany Department, Faculty of Science, Tanta University, Tanta 31527, Egypt
[i] Department of Chemical and Materials Engineering, Tamkang University, Tamsui, New Taipei 251, Taiwan
[j] Department of Chemistry, Faculty of Science, Universiti Brunei Darussalam, Gadong BE1410, Brunei
[k] Bioresource Engineering Research Group (BioERG), Department of Biotechnology, Faculty of Applied Sciences, Cape Peninsula University of Technology, Corner of Hanover, and Tennant Street, Zonnebloem, Cape Town 8000, South Africa
[l] Universiti Kuala Lumpur, Institute of Medical Science Technology, A1-1, Jalan TKS 1, Taman Kajang Sentral, 43000 Kajang, Selangor, Malaysia

ARTICLE INFO

Keywords:
Microalgae
Hydrogel
Phenol
Biohydrogen
Fermentation
Kinetic model

ABSTRACT

The potential of hydrogel immobilized microalgae-alginate beads to concurrently remove phenol and produce biohydrogen molecules from phenol-containing wastewaters with different phenol concentrations of 0.2 g/L to 1.2 g/L via dark fermentation had been successfully modelled and proven. Highest biohydrogen production and phenol removal were achieved at phenol concentration of 1.2 g/L. The lag phase of biohydrogen production increased with increasing of phenol concentration as the microalgal cells entailed a longer time to acclimatize in inhibitory medium of high phenol strength. The extended period for fermentation could also generate more biohydrogen molecules as compared with batch setup that was easily inhibited due to inadequate acclimatization allocation. Then, a new kinetic model was rederived from the modified Gompertz model and Andrew's inhibition model to describe the relationship between phenol concentration impacting the microalgal growth and subsequent biohydrogen production. Low concentration of phenol could serve as an alternative source of carbon to promote the microalgal growth and development; but high phenol concentration could hinder the growth of microalgae, afflicting the fermentative biohydrogen production. The rederived kinetic model was able to fit the experimental data for all phenol concentrations with coefficients of determination of greater than 0.95. This study had ultimately evidenced that the immobilized microalgae were able to ferment phenol and produce biohydrogen molecules simultaneously from phenol-containing wastewater.

* Corresponding authors at: HICoE-Centre for Biofuel and Biochemical Research, Institute of Sustainable Energy, Department of Fundamental and Applied Sciences, Universiti Teknologi PETRONAS, 32610 Seri Iskandar, Perak Darul Ridzuan, Malaysia (J.W. Lim). Department of Chemical Engineering, Faculty of Engineering and Industrial Technology, Silpakorn University, Nakhon Pathom 73000, Thailand (W. Kiatkittipong). Universiti Kuala Lumpur, Institute of Medical Science Technology, A1-1, Jalan TKS 1, Taman Kajang Sentral, 43000 Kajang, Selangor, Malaysia (W.-Y. Tong).
E-mail addresses: junwei.lim@utp.edu.my (J. Wei Lim), kiatkittipong_w@su.ac.th (W. Kiatkittipong), wytong@unikl.edu.my (W.-Y. Tong).
[1] Co-first authors.

https://doi.org/10.1016/j.molliq.2024.125157
Received 28 April 2024; Received in revised form 24 May 2024; Accepted 29 May 2024
Available online 31 May 2024

1. Introduction

Phenol is an aromatic organic compound and moderate soluble in water medium. It is usually found in the effluents of a variety of industries including pulp and paper (0.2–0.8 g/L), textile (0.10–0.15 g/L), petrochemicals (0.003–1.220 g/L), fiberglass manufacturing (0.400–2.564 g/L) and phenolic resin (1.2–1.6 g/L) [1–3]. Phenol and its derivatives are recognized to be dangerous to human beings, animals as well as aquatic life even at very low concentrations [4]. Owing to its toxicity, phenol poses severe acute and chronic impacts to human health and environment if disposed improperly. At fatal dosages, prolonged exposure can cause humans to experience respiratory arrest, tremor, muscle weakness, irregular breathing, and coma. Chronic exposure to phenols will lead to sudden loss of body weight, dizziness, a dark urine colour, diarrhea and anorexia [5–8]. In an aquatic environment, aquatic life will bioaccumulate phenol, affecting their growths by reducing their weights [8,9]. Besides, phenol can facilely react with chlorine to form carcinogenic chlorophenols [10]. Hence, phenol has been classified as priority water contaminants by the Environmental Protection Agency (EPA) in United States and the National Pollutant Release Inventory in Canada [8,1,10]. Phenol-containing wastewaters cannot be released into water bodies before undergoing the necessary treatments because of their hazardous, carcinogenic and characteristics which can have detrimental effects on many living organisms [11]. A strict limit of lower than 0.0005 g/L of phenol is allowed to be discharged into effluent because 1 g of phenol is suffice to kill a person, and it harms the aquatic life when the phenol concentrations are greater than 0.0010 g/L [12].

The removals of phenol from industrial wastewaters have raised significant concerns globally due to its high toxicity towards the environment and low in biodegradability [12,13]. Various techniques have been used to remove phenols from wastewaters including distillation, adsorption and extraction, chemical oxidation and electrochemical oxidation. However, these methods have faced several limitations. For instance, distillation technique has high energy demands which make it difficult to be used for large-scale operation. Besides, adsorption and extraction methods require a further disposal of the wastes produced after the reaction, such as the used adsorbent and liquid [8]. Chemical oxidation utilizes large amounts of strong oxidizing agents such as ozone and hydrogen peroxide, making it not economically viable. Although electrochemical oxidation does not require the use of chemicals, it is highly dependent on electrical energy and requires frequent replacement of the electrodes. On the other hand, biological treatment is another commonly utilized method to remove phenol that is inexpensive, environmentally friendly, and able to convert phenol into harmless end products [6,13,14]. Microbes such as microalgae (*Chlorella vulgaris* and *Scenedesmus* obliquus), fungi (Thielavia sp. and Debaryomyces sp.) and yeast (Rhodosporidium kratochvilovae HIMPA1) are usually involved in the phenolic treatment [14,15–18]. Generally, suspended microbes are used for degrading the pollutants that are present in wastewater. Nevertheless, the use of free cells has several disadvantages such as it is difficult to separate the free cells from the medium, low biodegradation efficiency, cell contamination and cell washing out in a continuous operational mode [4,19]. Furthermore, the biodegradation of phenol via biological method could be inhibited by the high concentration of phenol [20]. Thus, immobilization techniques such as cellular entrapment and adsorption have been explored to overcome such drawbacks. Immobilization techniques could form a barrier between cells and medium to protect and separate the cells from a direct contact with toxic effect of high concentration of phenol [21]. Besides, the immobilization could improve the survival rate of cells as well as its metabolic activities in treating wastewater. Sodium alginate, a naturally occurring polymer that is derived from brown seaweed such as *Laminaria* sp. *Sargassum* sp. and *Durvillaea* sp., has been widely used for cell immobilization to remove pollutants [22,23]. For instance, Solé and Matamoros [24] had immobilized microalgae in hydrogel alginate beads and utilized it to remove endocrine disrupting compounds from wastewater. Besides, Wang et al. [25] had produced immobilized *Zoogloea* sp. MFQ7-polyvinyl alcohol/sodium alginate with biochar gel beads to remove phenol, nitrate and manganese simultaneously. Gomes et al. [20] reported that the immobilized Candida tropicalis ATCC 750 onto cashew apple bagasse could tolerate an initial phenol concentration of greater than 1.4 g/L. They observed that the initial phenol concentration that showed the highest biodegradation of phenol by free and immobilized Candida tropicalis ATCC 750 were 0.45 g/L and 1.10 g/L, respectively.

Biodegradation of phenol with the production of biohydrogen molecules simultaneously is a green approach to treat wastewater and generate renewable energy. Hydrogen is considered as an alternative to replace fossil fuel because it merely produces water as a by-product after the combustion [26]. The common biological methods for producing biohydrogen molecules are direct and indirect bio-photolysis, dark fermentation and photo-fermentation. Dark fermentation is ubiquitously a preferred approach when comparing with others because it has low energy demand and can utilize organic wastes to produce biohydrogen while treating effluents. For instance, Patel et al. [27] had obtained the cumulative H_2 production of 3330 ± 5 mL/L from the cheese whey by Clostridium sp. IODB-O3 via dark fermentation. Murugan et al. [28] had examined the dark fermentative biohydrogen production from food wastewater, rice mill wastewater and sugar wastewater by Acinetobacter junii AH4, and the cumulative biohydrogen volumes obtained were 505.59 ± 2.52 mL/L, 354.19 ± 1.77 mL/L and 200.06 ± 1.00 mL/L, respectively. Immobilized microalgae-alginate beads could be used for simultaneous phenol removal and biohydrogen production via dark fermentation due to several reasons. The alginate matrix provides a stable and safe environment, protecting the entrapped microalgal biomass from the inhibitory and toxic effects of the phenol to ensure their continued viability [29]. Besides, immobilization matrix helps to create an anaerobic environment that promotes the production of biohydrogen via dark fermentation. The immobilization technique is also able to retain a high concentration of active microalgal biomass which improves the phenol removal efficiency and biohydrogen production.

The key objectives of this study are to evaluate the potential of hydrogel immobilized microalgae-alginate beads to produce biohydrogen molecules and remove phenols from phenol-containing wastewater via dark fermentation. Besides, the effect of phenol concentrations on the rates of biohydrogen productions was also described by using Andrew's inhibition model. Lastly, a new kinetic model that could predict the relationship between initial phenol concentration exerted on the growth of entrapped microalgal biomass and production of biohydrogen was developed, and subsequently validated from the experimental biohydrogen production data.

2. Methodology

2.1. Microalgal stock culture

Chlorella vulgaris species was employed in this study due to its potential in performing fermentative process to generate microalgal hydrogen product. Initially, a 500 mL volume of microalgal culture was introduced into a 5-L photobioreactor. This microalgal species was cultured in a sulfur-deprived medium in which constituting of 4.5 L of $NaNO_3$ (0.25 g/L), KH_2PO_4 (0.3375 g/L) and K_2HPO_4 (0.7875 g/L) to facilitate the later fermentative process. The photobioreactor was exposed to the continuous aeration by a compressed air unit at a rate of 1.0 L/min under the room temperature environment. Also, it is being illuminated with a cool and white fluorescent lamp at the light intensity of 60–70 μmol/m^2/s. The microalgae were cultured until it reached a stationary growth phase before being used for the subsequent fermentative experimental setups.

2.2. Hydrogel immobilized microalgae-alginate beads

Microalgal stock of 100 mL volume containing 0.125 g of microalgae was initially centrifuged at 5000 rpm for 10 min to obtain a concentrated microalgal flock. In preparing the hydrogel immobilized microalgae-alginate beads with 6 % w/v of sodium alginate concentration, the 3.0 g of sodium alginate was weighed and dissolved in 30 mL of distilled water. Then, the concentrated microalgal flock was added into sodium alginate solution and topped up with distilled water to attain a total final volume of 50 mL. This solution was then homogenized immediately. In producing the spherical beads, the homogenized solution mixture was dropped into 100 mL of 5 % w/v of $CaCl_2$ solution by using a peristaltic pump, connecting through a thin borosilicate glass dropper. Next, the hydrogel immobilized microalgae-alginate beads were kept in the similar $CaCl_2$ solution for 2 h with a gentle stirring to harden the beads. After that, the hydrogel immobilized microalgae-alginate beads were washed with tap water for several times to remove the excessive unpolymerized residue. Finally, the hydrogel immobilized microalgae-alginate beads of averagely 3 mm in diameter were used instantly for the biohydrogen production experiments via fermentative process.

2.3. Simulated phenol-containing wastewater medium

The simulated phenol-containing wastewater was prepared to contain these compounds: Phenol (0.2 g/L), NaCl (7 mg/L), $CaCl_2$ (4 mg/L), NH_4Cl (115 mg/L), KH_2PO_4 (15 mg/L), and $MgCl_2{\cdot}6H_2O$ (2 mg/L). Indeed, the concentrations of phenol were later varied to 0.4 g/L, 0.6 g/L, 0.8 g/L and 1.2 g/L. According to Ruiz-Marin et al. [30], this composition was well corresponded with the characteristics of real municipal wastewater.

2.4. Dark fermentative process

The dark fermentative biohydrogen production was conducted in a 200-mL of serum bottle with an additional 40 mL of unmarked volume. Each serum bottle was filled with 100 mL of wastewater medium and 50 mL of hydrogel immobilized microalgae-alginate beads. The headspace volume of serum bottle was left with 90 mL after filling with the wastewater medium and immobilized microalgae-alginate beads. Then, each content in serum bottle was purged with nitrogen gas for 20 min to eliminate the dissolved oxygen, while creating an anoxic environment for facilitating the dark fermentative process. The serum bottle was immediately and tightly closed with a 20-mm aluminium vial seal with Teflon septa and covered with aluminium foil, followed by a black cloth, to ensure that the fermentation was occurring in the absence of light. The serum bottle was placed on an orbital shaker with a rotary speed of 150 rpm at room temperature. The produced biohydrogen molecules in the headspace of serum bottle was analysed at every 24 h by withdrawing 1 mL volume from the headspace through the Teflon septa until there was no further increase in biohydrogen production. Thereafter, the wastewater medium containing hydrogel immobilized microalgae-alginate beads was purged with the nitrogen gas again prior to the begin of subsequent cycles of uses under the similar operational condition. These recyclable procedures continued until the biohydrogen productions had depleted from each wastewater medium. In verifying the reproducibility of biohydrogen production results, the standard deviations were also calculated from the duplicated experiments to confirm the consistency.

For achieving the extended period of biohydrogen production, these similar steps were repeated by replacing the 200-mL of serum bottle with 500-mL bottle. The headspace volume was at 350 mL after filling with the wastewater medium and immobilized microalgae-alginate beads. The bottle was immediately closed with a silicon septa cap after the purging with nitrogen gas. Likewise, this experiment was as well performed in duplicates for each concentration of phenol to ensure the consistency of data collected.

2.5. Analysis of biohydrogen

The biohydrogen sample was analysed by using the Perkin Elmer Clarus 580 Gas Chromatography unit with a Natural Gas Analyzer (GC-NGA). The GC-NGA was also coupled with thermal conductivity detector (TCD) to accurately detect and measure the volume of hydrogen gas. The temperatures were controlled as follows: Column oven at 110℃ and TCD at 200℃. Nitrogen was used as a carrier gas at a flowrate of 40 mL/min. A 1 mL of sample was withdrawn from the headspace by using a gas tight syringe and injected immediately into the GC-NGA for analysis. The calibration curve was early developed by injecting a series of known hydrogen volumes into the GC-NGA. The peak areas obtained were plotted against the hydrogen volumes, respectively. The linear equation of calibration curve attained was used to calculate the volumes of biohydrogen obtained during the experiments.

2.6. Analysis of phenol concentration

The direct photometric method by American Public Health Association (APHA) was used to determine the phenol concentration that presented in the wastewater medium [31]. Firstly, a 25 mL of distilled water as blank and a series of 25 mL of phenol standards that containing 1.0 mg/L, 2.0 mg/L, 3.0 mg/L, 4.0 mg/L and 5.0 mg/L were prepared in order to develop a calibration curve. Then, a 0.625 mL of 0.5 N of NH_4OH solution was added into the blank, phenol standards and samples each. The pH of each solution was adjusted to 7.9 ± 0.1 by using the phosphate buffer solution. After that, a 0.25 mL of 4-aminoantipyrine was added into each solution, followed by 0.25 mL of potassium ferricyanide solution. The solutions of blank, phenol standards and samples were made sure to mix well before adding every reagent. The solutions were transferred into the spectrometric cuvette each after 15 min, and the absorbance was read against the blank at 500 nm using the UV–Vis spectrophotometer. For constructing the calibration curve, the absorbance values obtained for phenol standards were plotted against the phenol concentrations, respectively. The phenol concentrations that presented in the wastewater samples were determined from the linear equation of calibration curve.

2.7. Kinetic model rederivation for the prediction of biohydrogen productions

Initially, the modified Gompertz model that is expressed in Equation (1) was employed to predict the cumulative biohydrogen production at time (t) from dark fermentation. The data of cumulative biohydrogen production at time (t) were collected experimentally in order to attain the following parameters from modelled prediction: H_{max} which is the maximum potential of biohydrogen yield (mL), R_{max} which is the maximum biohydrogen production rate (mL/h), t which is the arbitrary time of biohydrogen production (h) and λ which is the lag phase of biohydrogen production (h). Next, the parameter r in Equation (2) which is the rate of biohydrogen production (mL/h) was computed for each phenol concentration after all of the variables in Equation (1) were attained [32,33].

$$H = H_{max} \times \exp\{-\exp[\frac{2,71828 \times R_{max}}{H_{max}}(\lambda - t) + 1]\} \quad (1)$$

$$r = \frac{H_{max}}{\lambda + \frac{H_{max}}{R_{max}}} \quad (2)$$

Following that, the Andrew's inhibition model that is presented in Equation (3) was used to describe the dependence of r, biohydrogen production rate (mL/h) on S, the phenol concentration (g/L).

$$r = \frac{k \times S}{K_s + S + \frac{S^2}{K_i}} \tag{3}$$

In this case, k is the biohydrogen production rate constant (g/L), K_s is the half saturation constant (g/L) and K_i is the inhibition constant (g/L). All these kinetic parameters, H_{max}, R_{max}, λ, r, k, K_s and K_i could be determined by fitting the collected data into OriginPro 2022 software tool; and the correlation coefficient (R^2) values were subsequently evaluated together with the standard errors from fitting of models.

The modified Gompertz model from Equation (1) was used as a base to perform the rederivation of kinetic modelling in fitting the experimental biohydrogen data further. The rate of biohydrogen production could also be described by Equation (4) in which $Y_{H_2/x}$ is the yield coefficient of biohydrogen on biomass (mL/g), μ is the specific microalgae growth rate (1/h) and x_0 is the initial concentration of entrapped microalgae (g/L).

$$R = Y_{\frac{H_2}{x}} \times \mu \times x_0 \tag{4}$$

The substrate inhibition on biohydrogen production could be described by the Andrew's inhibition model associated to microalgal growth which is given in Equation (5).

$$\mu = \frac{\mu_{max} \times S}{K_s + S + \frac{S^2}{K_i}} \tag{5}$$

Where μ_{max} is the maximum biomass growth rate (1/h), S is the substrate concentration (g/L), K_s is the half-saturation constant (g/L) that denotes the substrate concentration when the growth rate is half of μ_{max} and K_i is the inhibition constant (g/L).

By substituting Equation (5) into Equation (4), the rate of biohydrogen production becomes:

$$R_{H_2} = Y_{H_2/X} \times \frac{\mu_{max} \times S}{k_s + S + \frac{S^2}{k_i}} \times x_0 \tag{6}$$

Assuming the rate of biohydrogen production in Equation (6) is the maximum biohydrogen production rate, which is known as R_{max} in modified Gompertz model, the Equation (7) is rederived by substituting Equation (6) into Equation (1).

$$H(t) = H_{max} \times \exp\{-\exp[\frac{e \times Y_{\frac{H_2}{x}} \times \frac{\mu_{max} \times S}{k_s + S + \frac{S^2}{k_i}} \times x_0}{H_{max}}(\lambda - t) + 1]\} \tag{7}$$

This Equation (7) can be rearranged as follows:

$$H(t) = H_{max} \times \exp\{-\exp[\frac{e \times Y_{\frac{H_2}{x}} \times \mu_{max} \times S \times x_0}{H_{max} \times (k_s + S + \frac{S^2}{k_i})}(\lambda - t) + 1]\} \tag{8}$$

Next, the yield coefficient of biohydrogen on biomass in Equation (8) is expressed as in Equation (9):

$$Y_{\frac{H_2}{x}} = \frac{\text{Hydrogen Produced (mL)}}{x - x_0} \tag{9}$$

The rearrangement will lead to the Equation (10) as follows:

$$x - x_0 = \frac{\text{Hydrogen Produced (mL)}}{Y_{\frac{H_2}{x}}} \tag{10}$$

Where x is the final biomass concentration (g/L) and x_0 is the initial biomass concentration (g/L).

The yield coefficient of biohydrogen on biomass can be related to the yield coefficient of biohydrogen on substrate and the yield coefficient of biomass on substrate. The yield coefficient of biohydrogen on substrate is presented in Equation (11).

$$Y_{\frac{H_2}{S}} = \frac{\text{Hydrogen Produced (mL)}}{S_0 - S} \tag{11}$$

The rearrangement will lead to the Equation (12) as follows:

$$S_0 - S = \frac{\text{Hydrogen Produced (mL)}}{Y_{\frac{H_2}{S}}} \tag{12}$$

Where S is the final substrate concentration (g/L) and S_0 is the initial substrate concentration (g/L).

The yield coefficient of biomass on substrate is expressed as below [34]:

$$Y_{\frac{x}{S}} = \frac{x - x_0}{S_0 - S} \tag{13}$$

The rearrangement will lead to the Equation (14) as follows:

$$Y_{\frac{x}{S}} \times (S_0 - S) = x - x_0 \tag{14}$$

Substituting Equation (12) into Equation (14), the difference in biomass becomes:

$$Y_{\frac{x}{S}} \times \frac{\text{Hydrogen Produced (mL)}}{Y_{\frac{H_2}{S}}} = x - x_0 \tag{15}$$

Substituting Equation (15) into Equation (9), it becomes:

$$Y_{\frac{x}{S}} \times \frac{\text{Hydrogen Produced (mL)}}{Y_{\frac{H_2}{S}}} = \frac{\text{Hydrogen Produced (mL)}}{Y_{\frac{H_2}{x}}} \tag{16}$$

The rearrangement will lead to the Equation (17) as follows:

$$Y_{\frac{H_2}{S}} = \frac{Y_{\frac{H_2}{S}}}{Y_{\frac{x}{S}}} \tag{17}$$

In fitting the experimental data of the yield coefficient of biohydrogen on substrate and the change of substrate into the equation, Equation (13) is substituted into Equation (17) and the yield coefficient of biohydrogen on biomass becomes:

$$Y_{\frac{H_2}{x}} = \frac{Y_{\frac{H_2}{S}}}{\frac{x - x_0}{S_0 - S}} \tag{18}$$

By substituting Equation (18) into Equation (8), the modified Gompertz model becomes:

$$H(t) = H_{max} \times \exp\{-\exp[\frac{e \times \frac{Y_{\frac{H_2}{S}}}{\frac{x - x_0}{S_0 - S}} \times \mu_{max} \times S \times x_0}{H_{max} \times (K_s + S + \frac{S^2}{K_i})}(\lambda - t) + 1]\} \tag{19}$$

The rearrangement will lead to the Equation (20) as follows:

$$H(t) = H_{max} \times \exp\{-\exp[\frac{e \times Y_{\frac{H_2}{S}} \times \mu_{max} \times S \times x_0}{H_{max} \times \frac{x - x_0}{S_0 - S} \times (K + S + \frac{S^2}{K_i})}(\lambda - t) + 1]\} \tag{20}$$

This rederived kinetic model can predict the relationship between biohydrogen production from microalgae and initial substrate concentration in the medium. The feasibility of model for current study is based on the following assumptions: (1) The initial concentration of microalgal biomass is same for all sets of alginate beads that are used for dark fermentative biohydrogen productions from phenol-containing wastewaters with different phenol concentrations. (2) The final microalgal biomass concentration is lower than the initial concentration due to the biomass detachment-cum-leakage from alginate beads. Therefore, the Equation (20) is finally corrected to as follows:

$$H(t) = H_{max} \times \exp\{-\exp[\frac{e \times Y_{H_2} \times \mu_{max} \times S \times x_0}{H_{max} \times \frac{x_0 - x}{S_0 - S} \times (K_s + S + \frac{S^2}{K_i})}(\lambda - t) + 1]\} \quad (21)$$

The kinetic parameters of H_{max}, R_{max}, μ_{max}, x, K_s, K_i and λ could be determined by fitting the collected data into OriginPro 2022 software tool; and the correlation coefficient (R^2) was subsequently evaluated together with the standard error from fitting of model.

3. Results and discussion

3.1. Dark fermentative biohydrogen productions in batches at different phenol concentrations

In this study, five different phenol concentrations in wastewater mediums ranging from 0.2–1.2 g/L were exploited as a sole carbon source to investigate its effect on producing biohydrogen molecules by hydrogel immobilized microalgae-alginate beads. Fig. 1 depicts the cumulative biohydrogen productions recorded from the first cycle of dark fermentative biohydrogen productions. The biohydrogen productions decreased stepwise when the phenol concentrations increased up to 0.8 g/L. According to Mamimin et al. [35], high phenol concentrations frequently led to the microalgal inhibitions in which reduced the metabolic productions of biohydrogen. However, the highest biohydrogen production was observed at phenol concentration of 1.2 g/L which was 18.07 ± 0.85 mL. From the trend, the biohydrogen production at phenol concentration of 1.2 g/L had started only after 96 h of lag phase. The production then increased gradually from 120 h to 240 h, before ratcheting up significantly after 240 h. In this case, the microalgae had experienced a stationary growth phase from 120 h to 240 h which was also plausibly the second acclimatization phase for the microalgae to alter its metabolic functions and thrive at high phenol concentration. The highest biohydrogen production was observed at a phenol concentration of 1.2 g/L as microalgal cells were able to adapt to the new environment gradually. The immobilized microalgal cells were undergoing two times of acclimatization processes to alter their metabolic activities to effectively utilize phenol as the substrates for biohydrogen production which led to the enhancement in biohydrogen production. Thereafter, the entrapped microalgae could utilize phenol as the substrate to maximize its biohydrogen production via the dark fermentation. Fig. 2 and Fig. 3 show the cumulative biohydrogen productions measured from the second cycle and third cycle of dark fermentative biohydrogen productions, respectively. In the second

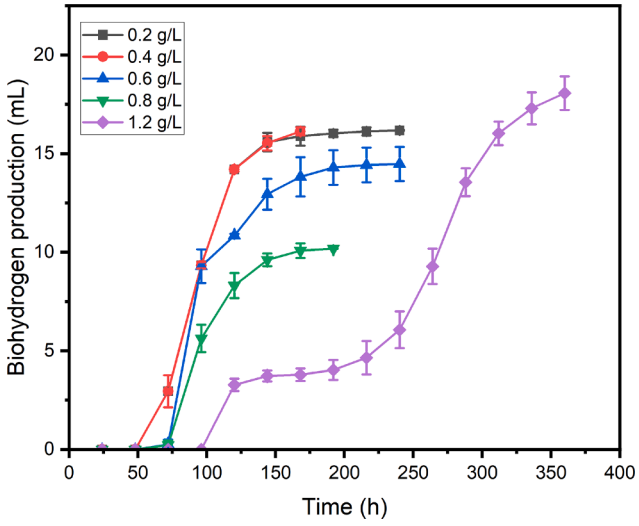

Fig. 1. First cycle of dark fermentative biohydrogen productions from hydrogel immobilized microalgae-alginate beads in phenol-containing wastewater mediums at different concentrations. Error bars represent the standard deviations.

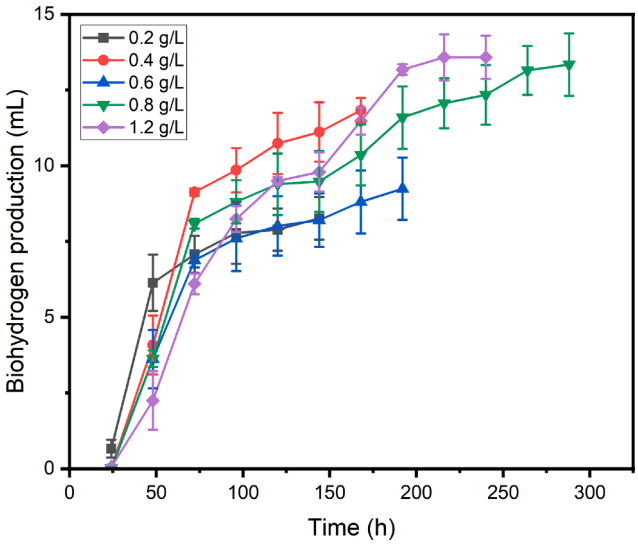

Fig. 2. Second cycle of dark fermentative biohydrogen productions from hydrogel immobilized microalgae-alginate beads in phenol-containing wastewater mediums at different concentrations. Error bars represent the standard deviations.

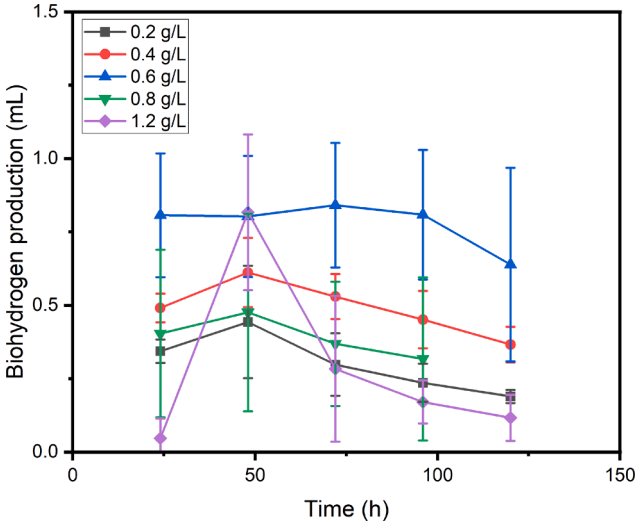

Fig. 3. Third cycle of dark fermentative biohydrogen productions from hydrogel immobilized microalgae-alginate beads in phenol-containing wastewater mediums at different concentrations. Error bars represent the standard deviations.

cycle, the highest biohydrogen productions from phenol concentrations of 0.8 g/L and 1.2 g/L were correspondingly at 13.34 ± 1.03 mL and 13.58 ± 0.71 mL. The lowest biohydrogen production was obtained at phenol concentration of 0.2 g/L which was 8.27 ± 0.70 mL, followed by phenol concentrations of 0.6 g/L at 9.24 ± 1.03 mL. Amidst the third cycle, the biohydrogen productions were decreasing drastically for all phenol concentrations which were varying merely from 0.40 mL to 0.90 mL.

Respectively, the phenol removals by hydrogel immobilized microalgae-alginate beads from each cycle are shown in Table 1. The phenol removals increased with increasing of phenol concentrations and decreased with increasing of cycles. The decrease of biohydrogen productions and phenol removals with increasing cycles may be due to the inhibition by entrapped microalgal cells by phenol. Moreover, the cell leakage from beads and adsorption of potential reaction products into the alginate matrix also could be the reasons that caused the decrease in

Table 1
Removal of phenol concentrations from each cycle during dark fermentation.

Phenol concentration (g/L)	Phenol removal (g/L)			Total phenol removal (g/L)
	First cycle	Second cycle	Third cycle	
0.2	0.0697 ± 0.0036	0.0364 ± 0.0036	0.0241 ± 0.0132	0.1302
0.4	0.0757 ± 0.0116	0.0896 ± 0.0040	0.0356 ± 0.0250	0.2009
0.6	0.1710 ± 0.0134	0.0965 ± 0.0036	0.0454 ± 0.0375	0.3129
0.8	0.2252 ± 0.0339	0.1647 ± 0.0045	0.0013 ± 0.0187	0.3912
1.2	0.4252 ± 0.0170	0.2145 ± 0.0009	0.0360 ± 0.0178	0.6757

phenol removals with increasing cycles of uses for dark fermentative biohydrogen productions [36,37]. The cell leakage from the beads would decrease the amount of active biomass entrapped in the alginate bead to metabolise phenol; and consequently, leading to the decrease in phenol removal efficiency. The adsorption of reaction products onto the alginate matrix would block the active sites of alginate beads. As a result, the available surface area of alginate beads for diffusion of phenol and degradation decreased. Several research studies had also found that phenol removal efficiencies declined as the number of cycles increased. Asimakoula et al. [37] reported that the phenol degradation efficiency of hydrogel alginate-immobilized *Pseudarthrobacter phenanthrenivorans* - Sphe3 decreased to lower than 75 % after five cycles. Basak et al. [38] studied the phenol degradation rate of hydrogel alginate-immobilized *Candida tropicalis* PHB5 that had reduced to 3.74 % after ten cycles. Furthermore from Table 1, the removals of phenol increased as the initial concentrations of phenol increased because the diffusion gradient of alginate beads increased with increasing initial phenol concentrations. The greater driving force at higher phenol concentrations would lead to the migration of more phenol molecules from the bulk solution into the alginate beads [11,21]. Then, more phenol molecules were fermented via metabolic degradation by the entrapped microalgae to produce more biohydrogen molecules. In the alginate beads, the microalgae were protected from the detrimental impacts of high phenol concentrations to maintain their metabolic activities. The alginate matrix also offered a stable environment to microalgae, prolonging their viability and activity. Besides, the high concentration of entrapped microalgae in the alginate beads may promote effective phenol uptake and breakdown in order to maximising biohydrogen production.

3.2. Kinetics for dark fermentative biohydrogen productions in batches at different phenol concentrations

Table 2 and Table 3 show the kinetic values of maximum biohydrogen production (H_{max}), maximum rate of biohydrogen production (R_{max}) and lag phase (λ) from each phenol concentration that were determined from the modified Gompertz model [Equation (1)] as well as the rate of biohydrogen production (r) that was obtained from [Equation (2)]. Based on the results, the modified Gompertz model could fit the experimental data from Fig. 1 and Fig. 2 well with the coefficient of determination (R^2) values of higher than 0.95 for all phenol-containing wastewater mediums. However, the modified Gompertz model was unable to fit the experimental data from cycle 3 (Fig. 3) due to insufficient data points. Moreover, it was observed in Table 2 that the time required for acclimatization by microalgae in the presence of phenol was directly correlated with the initial concentration of phenol in wastewater medium. The lag phase increased as the phenol concentration increased to over 0.4 g/L. According to Shahryari et al. [39] and Wen et al. [40], the exposure of microorganisms to high phenol concentration may change the structure of cell membrane and increase its permeability which could cause the loss of essential components; and ultimately, engendering cellular death. Thus, as the phenol concentration increased, the lag phase also increased because the microalgal cells required longer time to acclimatize towards the inhibitory effect exerted at greater phenol concentration. The maximum rates of biohydrogen productions (R_{max}) for phenol concentrations from 0.2 g/L to 0.6 g/L were in the range of 0.30 to 0.32 mL/h; and it started to decrease when the phenol concentrations were greater than 0.6 g/L. Lee et al. [41] also discovered the biohydrogen rate declined with increasing of phenol concentration. The maximum rates of biohydrogen productions were affected directly by the duration of acclimatization process by microalgae. As the phenol concentrations increased, the growths of microalgae and metabolisms would be inhibited. Thus, the microalgae required longer time to overcome and adapt to the inhibitory effect at higher phenol concentration. As a result, the maximum biohydrogen production occurred slower than that of at lower phenol concentrations where the acclimatization could transpire faster.

Table 2
Kinetic parameters derived from modified Gompertz model for first cycle of dark fermentative biohydrogen production by hydrogel immobilized microalgae-alginate beads at different concentrations of phenol-containing wastewater mediums.

Phenol concentration (g/L)	H_{max} (mL)	R_{max} (mL/h)	λ (h)	R^2	Adj-R^2
0.2	16.19	0.30	63.41	0.9995	0.9993
0.4	16.45	0.30	63.05	0.9995	0.9992
0.6	13.93	0.32	70.50	0.9846	0.9802
0.8	10.02	0.23	72.96	0.9972	0.9961
1.2	22.25	0.13	114.29	0.9913	0.9894

Table 3
Kinetic parameters derived from modified Gompertz model for second cycle of dark fermentative biohydrogen production by hydrogel immobilized microalgae-alginate beads at different concentrations of phenol-containing wastewater mediums.

Phenol concentration (g/L)	H_{max} (mL)	R_{max} (mL/h)	λ (h)	R^2	Adj-R^2
0.2	7.86	0.26	22.45	0.9881	0.9801
0.4	11.18	0.24	30.76	0.9902	0.9852
0.6	8.57	0.17	27.34	0.9843	0.9780
0.8	12.29	0.13	19.82	0.9537	0.9383
1.2	13.75	0.11	23.65	0.9761	0.9692

3.3. Extended period of dark fermentative biohydrogen productions at different phenol concentrations

Fig. 4 shows the cumulative biohydrogen productions under an extended period of dark fermentative processes by hydrogel immobilized microalgae-alginate beads in phenol-containing wastewater mediums at different concentrations. The highest volume of biohydrogen was obtained at phenol concentration of 1.2 g/L to the tune of 32.47 ± 1.06 mL, followed by phenol concentrations of 0.4 g/L and 0.8 g/L which were 28.57 ± 0.12 mL and 28.27 ± 0.67 mL, respectively. The biohydrogen productions attained at phenol concentrations of 0.2 g/L and 0.6 g/L were closed to each other, which were correspondingly at 24.89 ± 0.19 mL and 24.56 ± 0.85 mL. The differences among biohydrogen productions at phenol concentrations of 0.2 g/L and 0.6 g/L as well as 0.4 g/L and 0.8 g/L showed little variations which were merely at 0.30 ± 0.06 mL for each. Furthermore, the lag phases for biohydrogen productions under an extended period followed the trends as observed for the first cycle in Fig. 1. The lag phases generally increased with increasing of phenol concentrations as longer times were needed by microalgae to acclimatize in the presence of inhibitory effects exerted by phenol at higher concentrations.

Table 4 shows the summary of biohydrogen productions under the extended period of dark fermentation with respect to the remediations of

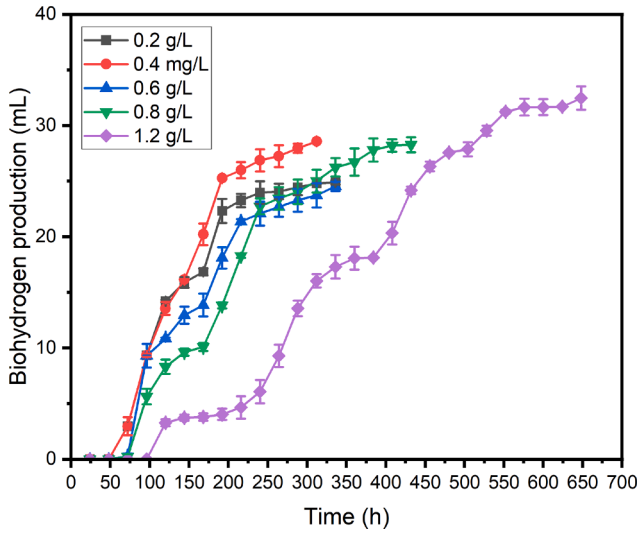

Fig. 4. Extended period of dark fermentative biohydrogen productions from hydrogel immobilized microalgae-alginate beads in phenol-containing wastewater mediums at different concentrations. Error bars represent the standard deviations.

Table 4
Biohydrogen productions and treatments of phenol-containing wastewater mediums at different concentrations by hydrogel immobilized microalgae-alginate beads at extended period of dark fermentation.

Phenol concentration (g/L)	Biohydrogen production (mL)	Final phenol concentration (g/L)	Total phenol removal (g/L)	Phenol removal efficiency (%)
0.2	24.89 ± 0.19128	0.07 ± 0.0132	0.13	65.2
0.4	28.57 ± 0.11791	0.20 ± 0.0251	0.20	50.0
0.6	24.56 ± 0.4225	0.29 ± 0.0375	0.31	52.2
0.8	28.27 ± 0.6729	0.41 ± 0.0187	0.39	48.9
1.2	32.47 ± 1.0622	0.52 ± 0.0178	0.68	56.3

phenol-containing wastewater mediums. The phenol removal efficiencies at initial concentrations of 0.4 g/L and 1.2 g/L were varying from 48.00 % to 57.00 %, respectively, while the highest phenol removal efficiency was achieved at the lowest phenol concentration of 0.2 g/L. Xiao et al. [15] had studied the biodegradation of phenol in BG-11 medium by using Chlorella vulgaris. During the study, Chlorella vulgaris was found able to tolerate the phenol concentrations up to 0.8 g/L. Besides, the *Chlorella vulgaris* had achieved the phenol degradation efficiencies of 100 % and 56 % for phenol concentrations of 0.1 g/L and 0.3 g/L, respectively. However, the degradation of phenol decreased to lower than 10 % when the phenol concentration was increased to 0.8 g/L. The authors suggested that the lower phenol removal efficiency at higher phenol concentration may be due to the inhibition of degradation capacity of microalgae at high concentration of phenol. The current study had demonstrated a better removal efficiency of phenol, primary due to the shield offered by hydrogel alginate beads that had abated the inhibitory effects of phenol when the wastewater medium was diffusing towards the inner layers of beads with immobilized microalgae. In this regard, this had enabled the immobilized microalgae to still perform fermentative process in generating biohydrogen rather than being totally inhibited at 0.8 g/L of phenol as reported by Xiao et al. [15] employing the same species of microalgae, namely, *Chlorella vulgaris*.

3.4. Kinetics for extended period of dark fermentative biohydrogen productions at different phenol concentrations

Table 5 presents the modelling results for maximum biohydrogen productions (H_{max}), maximum rates of biohydrogen productions (R_{max}) and lag phases (λ) attained from each phenol concentration that were determined by modified Gompertz model [Equation (1)]. On the other hand, the predicted rates of biohydrogen productions (r_p) that were modelled from [Equation (2)] are shown in Table 6. The modified Gompertz model could fit the experimental data from Fig. 4 adequately with the coefficient of determination (R^2) values of greater than 0.97 for all phenol concentrations. Also, according to Table 5, the lag phases for biohydrogen productions at phenol concentrations from 0.2 g/L to 0.4 g/L were varying from 53.6 h to 58.0 h; and it had prolonged significantly as the phenol concentration was increased to 1.2 g/L. Next, the maximum rates of biohydrogen productions declined as the phenol concentrations were increased beyond 0.4 g/L. The rates of biohydrogen productions (r_p) as calculated from Equation (2) had the same trend with the maximum rates of biohydrogen productions (R_{max}). For verification, the percentage errors between predicted and experimental rates of biohydrogen productions are indicated in Table 6. In this case, the percentage errors were lower than 15 % for all phenol concentrations, which had signified that the predicted rates of biohydrogen productions were accurately modelled.

The values of kinetic parameters, namely, H_{max} and λ in Table 5, that were determined from the modified Gompertz model were used to fit into the rederived model of Equation (21) together with the experimental data from Fig. 4. The results which are revealed in Table 7 had demonstrated that the rederived model could fit the experimental data thoroughly with coefficient of determination (R^2) values of more than 0.97 for each of phenol-containing wastewater mediums. The maximum specific microalgal growth rates (μ_{max}) were found decreasing with the increase of concentrations of phenol. Microalgae primarily use carbon dioxide for a variety of metabolic activities [42]. However, they can also utilize organic carbon as their carbon source when the availability of carbon dioxide is limited. According to Lika et al. [44] and Das et al. [45], the microalgae could metabolize phenol into simple organic products such as pyruvate and carbon dioxide that may subsequently help to promote the biomass growth. In this study, phenol was the only source of carbon in the medium, stimulating the microalgal cells to produce carbon reserves in order to meet its carbon requirements for cellular structure and maintain their stability [43]. At low concentrations, microalgal cells were less inhibited by phenol. Thus, microalgae could metabolize and use phenol as an alternative source of carbon to promote its cellular growths and developments [43]. With sufficient amount of substrates, microalgae could utilize phenol efficiently and promote the growth of biomass. Thus, higher specific biomass growth rates were observed at lower phenol concentrations, leading to the increment of concentrations of entrapped microalgal biomass. On the other hand, at high phenol concentration could hinder the growth of microalgae, leading to the reduction in specific biomass growth rate because phenol would destroy the photosynthetic pigment and membrane bound organelles of the cells [46]. Therefore, the amount of

Table 5
Kinetic parameters derived from modified Gompertz model for extended period of dark fermentative biohydrogen productions by hydrogel immobilized microalgae-alginate beads at different concentrations of phenol-containing wastewater mediums.

Phenol concentration (g/L)	H_{max} (mL)	R_{max} (mL/h)	λ (h)	R^2	Adj-R^2
0.2	24.99	0.19	53.65	0.9876	0.9854
0.4	28.84	0.21	58.01	0.9930	0.9916
0.6	24.83	0.15	55.74	0.9751	0.9706
0.8	29.51	0.13	72.27	0.9868	0.9851
1.2	39.35	0.10	162.40	0.9922	0.9914

Table 6
Validation of dark fermentative biohydrogen production rates by hydrogel immobilized microalgae-alginate beads at different concentrations of phenol-containing wastewater mediums under extended period.

Phenol concentration (g/L)	Predicted rate of biohydrogen, r_p (mL/h)	Experimental rate of biohydrogen, r_e (mL/h)	Percentage error (%)
0.2	0.13	0.1184 ± 0.0010	8.9
0.4	0.14	0.1200 ± 0.0078	14.3
0.6	0.10	0.0968 ± 0.0111	3.2
0.8	0.09	0.0850 ± 0.0019	5.6
1.2	0.06	0.0577 ± 0.0002	3.8

Table 7
Kinetic parameters derived from the new formulated model [Equation (21)] for extended period of dark fermentative biohydrogen productions by hydrogel immobilized microalgae-alginate beads at different concentrations of phenol-containing wastewater mediums.

Phenol concentrations (g/L)	μ_{max} (1/h)	x (g/L)	R^2	Adj-R^2
0.2	0.18	0.31	0.9876	0.9854
0.4	0.15	0.39	0.9930	0.9916
0.6	0.16	0.34	0.9751	0.9706
0.8	0.14	0.36	0.9868	0.9851
1.2	0.06	0.79	0.9922	0.9914

entrapped biomass decreased due to the inhibition of phenol at higher concentration and lower the specific biomass growth rate. Besides, the final concentrations of entrapped active microalgal biomass for phenol concentrations from 0.2 g/L to 0.8 g/L were anticipated to vary from 0.30 g/L to 0.39 g/L, respectively, while the phenol concentration of 1.2 g/L had retained the highest final concentration of entrapped active microalgal biomass at 0.79 g/L. At phenol concentrations from 0.2 g/L to 0.8 g/L, the specific biomass growth rates were all higher than that of 1.2 g/L of phenol, leading to the increases of entrapped biomass concentrations and densities of microalgal cells. The increases in cell densities within the beads would restrict the nutrient diffusions from the medium into the beads, resulting in the nutrients starvation and potentially death of microalgae because the microalgae may not have sufficient nutrients to support its growths and metabolisms. Moreover, the rapid increases in entrapped biomass concentrations would also exert mechanical stresses on alginate polymeric matrix that led to the expansion and deformation of alginate beads. Consequently, some microalgal cells may be released from alginate beads into the medium which would significantly decrease the entrapped active biomass concentrations [47]. Therefore, these rationalized the final concentrations of entrapped active microalgal biomasses for phenol concentrations from 0.2 g/L to 0.8 g/L were lower than that of 1.2 g/L.

The Andrew's inhibition model of Equation (3) was then employed to describe the relationship between rate of biohydrogen production and substrate concentration. The parameter of inhibition constant (K_i) was obtained by fitting the rates of biohydrogen productions that were determined using Equation (2) and phenol concentrations used in this study. The Equation (22) below shows the results achieved with a high coefficient of determination (R^2) value of 0.9865.

$$r = \frac{3.80612 \times S}{4.07376 + S + \frac{S^2}{0.0213}} R^2 = 0.9865 \quad (22)$$

The inhibition constant (K_i) obtained in this study was at 0.0213 g/L. Geng et al. [48] found that the inhibition constant of phenol for Bacteria strain EDP3 was at 0.0580 g/L. Das et al. [45] reported that the inhibition constant of phenol for *Chlorella pyrenoidosa* (NCIM2738) in the phenol-containing nutrient medium and the refinery wastewater were at 0.0245 g/L and 0.0105 g/L, respectively. The obtained K_i value was lower than that of Bacteria strain EDP3, but very close to the *Chlorella pyrenoidosa* (NCIM2738) microalgae in the phenol-containing nutrient wastewater. A lower K_i value suggested that the microalgae were more sensitive towards the substrate inhibition, which also indicated that the microalgae growth rate would be inhibited even at low phenol concentration [45].

4. Conclusions

The potential of hydrogel immobilized microalgae-alginate beads to remove phenol and produce biohydrogen molecules simultaneously from phenol-containing wastewater with different phenol concentrations via dark fermentation had been evidenced. The immobilized microalgae could tolerate the phenol concentration up to 1.2 g/L, and the highest biohydrogen was achieved at this phenol concentration. Besides, the lag phases of biohydrogen productions increased with increasing of phenol concentrations as the microalgae required longer times to acclimatize towards higher phenol concentrations. The removals of phenol increased as the initial concentrations of phenol increased due to the increase in diffusion gradient of alginate beads, leading to more phenols could reach the inner layers of alginate beads for undergoing degradation by fermentative immobilized microalgae. The extended period of fermentation had successfully produced more biohydrogen molecules as opposed to the batch setup of similar phenol-containing wastewater. The modified Gompertz model, rederived kinetic model and Andrew's inhibition model were successfully validated by fitting the experimental data of biohydrogen productions from phenol-containing wastewaters with different phenol concentrations by hydrogel immobilized-microalgae alginate beads, having the coefficient of determination (R^2) values of more than 0.95. The future research is recommended to focus on immobilization of microalgae with activated sludge as the immobilized microalgae-bacteria system has higher tolerance towards toxicity of phenol. The incorporation of activated sludge and microalgae could minimize the inhibition of phenol on microalgae, reducing the lag phase for producing biohydrogen and increasing the phenol removal efficiently. The parameters such as pH and ratio of microalgae and activated sludge could be investigated to maximize the phenol removal and biohydrogen production simultaneously.

CRediT authorship contribution statement

Jia Min Woon: Writing – original draft, Investigation, Formal analysis, Data curation, Conceptualization. **Kuan Shiong Khoo:** Writing – review & editing, Funding acquisition, Formal analysis, Data curation, Conceptualization. **Mohsin Kazi:** Writing – review & editing, Funding acquisition. **Mohammad Nur-e-Alam:** Writing – review & editing, Funding acquisition. **Nurul Tasnim Sahrin:** Writing – review & editing, Investigation. **Jun Wei Lim:** Writing – original draft, Formal analysis, Data curation, Conceptualization. **Worapon Kiatkittipong:** Writing – review & editing, Investigation, Funding acquisition, Formal analysis, Conceptualization. **Sameh S. Ali:** Writing – review & editing, Formal analysis, Data curation. **Chii-Dong Ho:** Writing – original draft, Investigation. **Anwar Usman:** Writing – review & editing, Methodology. **Boredi Silas Chidi:** Writing – review & editing, Formal analysis. **Woei-Yenn Tong:** Writing – review & editing, Methodology, Investigation, Formal analysis.

Declaration of competing interest

The authors declare that they have no known competing financial interests or personal relationships that could have appeared to influence the work reported in this paper.

Data availability

Data will be made available on request.

Acknowledgements

This research is financially supported by Thailand Science Research and Innovation (TSRI) National Science, Research and Innovation Fund (NSRF) (Fiscal Year 2024). The authors would like to extend their sincere appreciation to the Researchers Supporting Project Number (RSPD2024R994), King Saud University, Riyadh, Saudi Arabia. We would also like to acknowledge the support provided by National Science and Technology Council (NSTC) International Internship Pilot Program for Woon Jia Min as the intern for the Department of Chemical Engineering and Materials Science, Yuan Ze University (Taiwan). One of the authors (Kuan Shiong Khoo) would like to gratefully acknowledge the work supported and financially funded by National Science and Technology Council, Taiwan (Project number: NSTC112-2222-E-155-005) and Department of Chemical Engineering and Materials Science, Yuan Ze University, Taiwan under New Faculty Research Start-Up Fund Scheme (Project no: 303014-1 and 303014-2).

References

[1] Y.H. Fseha, J. Shaheen, B. Sizirici, Phenol contaminated municipal wastewater treatment using date palm frond biochar: Optimization using response surface methodology, Emerg. Contam 9 (1) (Mar. 2023) 100202, https://doi.org/10.1016/J.EMCON.2022.100202.

[2] D.M. Naguib, N.M. Badawy, Phenol removal from wastewater using waste products, J. Environ. Chem. Eng 8 (1) (Feb. 2020) 103592, https://doi.org/10.1016/J.JECE.2019.103592.

[3] M.C. Tomei, D.M. Angelucci, E. Clagnan, L. Brusetti, Anaerobic biodegradation of phenol in wastewater treatment: achievements and limits, doi: 10.1007/s00253-021-11182-5/Published.

[4] Y. Jiang, T. Deng, Y. Shang, K. Yang, H. Wang, Biodegradation of phenol by entrapped cell of Debaryomyces sp. with nano-Fe3O4 under hypersaline conditions, Int. Biodeterior. Biodegradation 123 (Sep. 2017) 37–45, https://doi.org/10.1016/J.IBIOD.2017.05.029.

[5] A. Idris, W. Suzana, Effect of sodium alginate concentration, bead diameter, initial pH and temperature on lactic acid production from pineapple waste using immobilized Lactobacillus delbrueckii, Process. Biochemistry 41 (5) (2006) 1117–1123, https://doi.org/10.1016/j.procbio.2005.12.002.

[6] L.G.C. Villegas, N. Mashhadi, M. Chen, D. Mukherjee, K.E. Taylor, N. Biswas, A Short Review of Techniques for Phenol Removal from Wastewater, Curr. Pollut. Rep., vol. 2, no. 3. Springer, pp. 157–167, Sep. 01, 2016. doi: 10.1007/s40726-016-0035-3.

[7] E. Bazrafshan, F. Kord Mostafapour, H. Jafari Mansourian, Phenolic compounds: health effects and its removal from aqueous environments by low cost adsorbents, Health Scope, vol. 2, no. 2, pp. 65–66, Jul. 2013, doi: 10.17795/jhealthscope-12993.

[8] K.A. Mohamad Said, A F. Ismail, Z. Abdul Karim, M.S. Abdullah, A. Hafeez, A review of technologies for the phenolic compounds recovery and phenol removal from wastewater, Process Safety Environ. Protect., vol. 151, pp. 257–289, Jul. 2021, doi: 10.1016/J.PSEP.2021.05.015.

[9] A.A. Gami, M.Y. Shukor, K.A. Khalil, F.A. Dahalan, A. Khalid, S.A. Ahmad, Phenol and its toxicity, J. Environ. Microbiol. Toxicol. 2 (1) (Jul. 2014) 11–23, https://doi.org/10.54987/jemat.v2i1.89.

[10] R.M. Zahir, H. Hassan, A.A. Nagoor Gunny, Application of OPEFB fibre based electrode in microbial fuel cell system for electricity generation and chlorophenol degradation, in: IOP Conference Series: Earth and Environmental Science, IOP Publishing Ltd, May 2021. doi: 10.1088/1755-1315/765/1/012096.

[11] A.S. Khan, et al., Preparation of sustainable activated carbon-alginate beads impregnated with ionic liquid for phenol decontamination, J. Clean. Prod 321 (Oct. 2021) 128899, https://doi.org/10.1016/J.JCLEPRO.2021.128899.

[12] M.J. Khan et al., Wastewater Treatment Using Membrane Bioreactor Technologies: Removal of Phenolic Contaminants from Oil and Coal Refineries and Pharmaceutical Industries, Polymers, vol. 16, no. 3. Multidisciplinary Digital Publishing Institute (MDPI), Feb. 01, 2024. doi: 10.3390/polym16030443.

[13] V. Sridevi, M.V.V Chandana Lakshmi, M. Manasa, M. Sravani, Metabolic pathways for the biodegradation of phenol, 2012, [Online]. Available: https://www.researchgate.net/publication/268382828.

[14] N. Panigrahy, A. Priyadarshini, M.M. Sahoo, A.K. Verma, A. Daverey, N.K. Sahoo, A comprehensive review on eco-toxicity and biodegradation of phenolics: Recent progress and future outlook, Environ. Technol. Innov 27 (Aug. 2022) 102423, https://doi.org/10.1016/J.ETI.2022.102423.

[15] M. Xiao, et al., Characterization of cometabolic degradation of p-cresol with phenol as growth substrate by Chlorella vulgaris, Bioresour. Technol 281 (Jun. 2019) 296–302, https://doi.org/10.1016/J.BIORTECH.2019.02.079.

[16] A. Papazi, M. Karamanli, K. Kotzabasis, Comparative biodegradation of all chlorinated phenols by the microalga Scenedesmus obliquus — The biodegradation strategy of microalgae, J. Biotechnol 296 (Apr. 2019) 61–68, https://doi.org/10.1016/J.JBIOTEC.2019.03.010.

[17] A. Patel, K. Sartaj, N. Arora, V. Pruthi, P.A. Pruthi, Biodegradation of phenol via meta cleavage pathway triggers de novo TAG biosynthesis pathway in oleaginous yeast, J. Hazard. Mater 340 (Oct. 2017) 47–56, https://doi.org/10.1016/J.JHAZMAT.2017.07.013.

[18] R. Mtibaà, et al., Biodegradation and toxicity reduction of nonylphenol, 4-tert-octylphenol and 2,4-dichlorophenol by the ascomycetous fungus Thielavia sp HJ22: Identification of fungal metabolites and proposal of a putative pathway, Sci. Total Environ. 708 (Mar. 2020) 135129, https://doi.org/10.1016/J.SCITOTENV.2019.135129.

[19] M.F. Bergero, G.I. Lucchesi, Immobilization of Pseudomonas putida A (ATCC 12633) cells: A promising tool for effective degradation of quaternary ammonium compounds in industrial effluents, Int. Biodeterior. Biodegradation 100 (May 2015) 38–43, https://doi.org/10.1016/J.IBIOD.2015.02.004.

[20] N.C. Gomes, A.C. De Macedo, Á.D. Teles Pinheiro, M.V. Ponte Rocha, Phenol biodegradation by Candida tropicalis ATCC 750 immobilized on cashew apple bagasse, J. Environ. Chem. Eng., vol. 7, no. 3, p. 103076, Jun. 2019, doi: 10.1016/J.JECE.2019.103076.

[21] B. Ruan, et al., Immobilization of Sphingomonas sp. GY2B in polyvinyl alcohol–alginate–kaolin beads for efficient degradation of phenol against unfavorable environmental factors, Ecotoxicol. Environ. Saf 162 (Oct. 2018) 103–111, https://doi.org/10.1016/J.ECOENV.2018.06.058.

[22] A. Kumar, A. Sood, S.S. Han, Poly (vinyl alcohol)-alginate as potential matrix for various applications: A focused review, Carbohydr. Polym 277 (Feb. 2022) 118881, https://doi.org/10.1016/J.CARBPOL.2021.118881.

[23] E.J. Stobel Christy, A. Rajeswari, A. Pius, Biopolymer applications in cosmeceutical industries, Biopolym. Industr. Appl., pp. 219–243, Jan. 2021, doi: 10.1016/B978-0-12-819240-5.00009-2.

[24] A. Solé, V. Matamoros, Removal of endocrine disrupting compounds from wastewater by microalgae co-immobilized in alginate beads, Chemosphere 164 (Dec. 2016) 516–523, https://doi.org/10.1016/J.CHEMOSPHERE.2016.08.047.

[25] Y. Wang, J. Su, A. Ali, Q. Chang, Y. Bai, Z. Gao, Enhanced nitrate, manganese, and phenol removal by polyvinyl alcohol/sodium alginate with biochar gel beads immobilized bioreactor: Performance, mechanism, and bacterial diversity, Bioresour. Technol 348 (Mar. 2022) 126818, https://doi.org/10.1016/J.BIORTECH.2022.126818.

[26] N. Rashid, K. Lee, Q. Mahmood, Bio-hydrogen production by Chlorella vulgaris under diverse photoperiods, Bioresour. Technol 102 (2) (Jan. 2011) 2101–2104, https://doi.org/10.1016/J.BIORTECH.2010.08.032.

[27] A.K. Patel, N. Vaisnav, A. Mathur, R. Gupta, D.K. Tuli, Whey waste as potential feedstock for biohydrogen production, Renew. Energy 98 (Dec. 2016) 221–225, https://doi.org/10.1016/J.RENENE.2016.02.039.

[28] R.S. Murugan, et al., Dark fermentative biohydrogen production by Acinetobacter junii-AH4 utilizing various industry wastewaters, Int. J. Hydrogen. Energy 46 (20) (Mar. 2021) 11297–11304, https://doi.org/10.1016/J.IJHYDENE.2020.07.073.

[29] S.C. Martins, C.M. Martins, L.M. Fiúza, S.T. Santaella, Immobilization of microbial cells: A promising tool for treatment of toxic pollutants in industrial wastewater, Afr. J. Biotechnol 12 (28) (Jul. 2013) 4412–4418, https://doi.org/10.5897/ajb12.2677.

[30] A. Ruiz-Marin, Y. Canedo-López, P. Chávez-Fuentes, Biohydrogen production by Chlorella vulgaris and Scenedesmus obliquus immobilized cultivated in artificial wastewater under different light quality, AMB. Express 10 (1) (2020) 191, https://doi.org/10.1186/s13568-020-01129-w.

[31] Standard Methods for the Examination of Water and Wastewater, 1999.

[32] S. Pouresmaeil, M. Nosrati, S. Ebrahimi, Operating control for enrichment of hydrogen-producing bacteria from anaerobic sludge and kinetic analysis for vinasse inhibition, J. Environ. Chem. Eng 7 (3) (Jun. 2019), https://doi.org/10.1016/j.jece.2019.103090.

[33] J. Wang, W. Wan, The effect of substrate concentration on biohydrogen production by using kinetic models, Sci. China. B. Chem 51 (11) (Nov. 2008) 1110–1117, https://doi.org/10.1007/s11426-008-0104-6.

[34] M.S. Islam, K.M.A. Kabir, J. Tanimoto, B.B. Saha, Study on Spirulina platensis growth employing non-linear analysis of biomass kinetic models, Heliyon 7 (10) (Oct. 2021), https://doi.org/10.1016/j.heliyon.2021.e08185.

[35] C. Mamimin, P. Thongdumyu, A. Hniman, P. Prasertsan, T. Imai, S. O-Thong, Simultaneous thermophilic hydrogen production and phenol removal from palm oil mill effluent by Thermoanaerobacterium-rich sludge, Int. J. Hydrogen. Energy 37 (20) (Oct. 2012) 15598–15606, https://doi.org/10.1016/J.IJHYDENE.2012.04.062.

[36] C.E. Paisio, M.A. Talano, P.S. González, C. Magallanes-Noguera, M. Kurina-Sanz, E. Agostini, Biotechnological tools to improve bioremediation of phenol by Acinetobacter sp. RTE1.4, Environ. Technol 37 (18) (Sep. 2016) 2379–2390, https://doi.org/10.1080/09593330.2016.1150352.

[37] S. Asimakoula, O. Marinakos, E. Tsagogiannis, and A. I. Koukkou, Phenol Degradation by Pseudarthrobacter phenanthrenivorans Sphe3, Microorganisms, vol. 11, no. 2, Feb. 2023, doi: 10.3390/microorganisms11020524.

[38] B. Basak, B. Bhunia, A. Dey, Studies on the potential use of sugarcane bagasse as carrier matrix for immobilization of Candida tropicalis PHB5 for phenol biodegradation, Int. Biodeterior. Biodegrad. 93 (Sep. 2014) 107–117, https://doi.org/10.1016/J.IBIOD.2014.05.012.

[39] S. Shahryari, H.S. Zahiri, K. Haghbeen, L. Adrian, K.A. Noghabi, High phenol degradation capacity of a newly characterized Acinetobacter sp. SA01: Bacterial cell viability and membrane impairment in respect to the phenol toxicity, Ecotoxicol. Environ. Saf 164 (Nov. 2018) 455–466, https://doi.org/10.1016/J.ECOENV.2018.08.051.

[40] Y. Wen, C. Li, X. Song, Y. Yang, Biodegradation of phenol by rhodococcus sp. Strain SKC: Characterization and kinetics study, Molecules 25 (16) (Aug. 2020), https://doi.org/10.3390/molecules25163665.

[41] D.J. Lee, J. Tai, S.S. Adav, A. Su, Harvesting biohydrogen from toxic wastewater using isolated strain, Int. J. Hydrogen. Energy 36 (21) (Oct. 2011) 13907–13913, https://doi.org/10.1016/J.IJHYDENE.2011.03.053.
[42] M. Molazadeh, H. Ahmadzadeh, H. R. Pourianfar, S. Lyon, P.H. Rampelotto, The use of microalgae for coupling wastewater treatment with CO2 biofixation, Front. Bioeng. Biotechnol., vol. 7, no. MAR. Frontiers Media S.A., 2019. doi: 10.3389/fbioe.2019.00042.
[43] S.B.M. Radziff et al., Potential application of algae in biodegradation of phenol: A review and bibliometric study, Plants, vol. 10, no. 12. MDPI, Dec. 01, 2021. doi: 10.3390/plants10122677.
[44] K. Lika, I.A. Papadakis, Modeling the biodegradation of phenolic compounds by microalgae, J. Sea. Res 62 (2–3) (Aug. 2009) 135–146, https://doi.org/10.1016/J.SEARES.2009.02.005.
[45] B. Das, T.K. Mandal, S. Patra, A comprehensive study on Chlorella pyrenoidosa for phenol degradation and its potential applicability as biodiesel feedstock and animal feed, Appl. Biochem. Biotechnol 176 (5) (Jul. 2015) 1382–1401, https://doi.org/10.1007/s12010-015-1652-9.
[46] K. Cho, et al., Use of phenol-induced oxidative stress acclimation to stimulate cell growth and biodiesel production by the oceanic microalga Dunaliella salina, Algal. Res 17 (Jul. 2016) 61–66, https://doi.org/10.1016/J.ALGAL.2016.04.023.
[47] T.T. Nazos, D.F. Ghanotakis, Biodegradation of phenol by alginate immobilized Chlamydomonas reinhardtii cells, Arch. Microbiol 203 (9) (Nov. 2021) 5805–5816, https://doi.org/10.1007/s00203-021-02570-6.
[48] A. Geng, A.E.W. Soh, C.J. Lim, L.C.T. Loke, Isolation and characterization of a phenol-degrading bacterium from an industrial activated sludge, Appl. Microbiol. Biotechnol 71 (5) (Aug. 2006) 728–735, https://doi.org/10.1007/s00253-005-0199-z.